NIAC Phase 1 Final Report

Direct probe of dark energy interactions with a Solar System laboratory

December 28, 2018

Prepared by
Nan Yu, NIAC Fellow
Collaborators: Sheng-wey Chiow, Jérôme Gleyzes, Phil Bull, Olivier Doré, Jason Rhodes, Jeffrey Jewell, and Eric Huff
Jet Propulsion Laboratory, California Institute of Technology
Holger Müller
University of California, Berkeley

Jet Propulsion Laboratory
4800 Oak Grove Drive
MS 298-310
Pasadena, CA 91109-8099
nan.yu@jpl.nasa.gov

Jet Propulsion Laboratory
California Institute of Technology

Table of Contents

1. Introduction 2
   1.1 The most important science question in cosmology 2
   1.2 Challenges in direct detection of dark energy scalar fields 4
   1.3 Innovative approaches and significance 4
2. Enabling Technology – Atom Interferometry 5
   2.1 Laser cooling and light pulse atom interferometer 5
   2.2 Atomic test mass for the mission concept 7
   2.3 State of AI developments for space 8
3. Measurement Concept and Mission architecture 9
   3.1 Measurement strategy – Tracelessness test for the unknown force 9
   3.2 Robust measurement configuration 10
   3.3 Measurement of gradient tensor and trace 11
   3.4 Drag-free inertial references 12
   3.5 Laser interferometer ranging 13
   3.6 Choice of baseline length 14
   3.7 Choice of mission trajectories 17
4. Technology Feasibilities 18
   4.1 Atomic inertial reference instrument 18
      4.1.1 AI sensitivity 18
      4.1.2 Ultra-cold atom source 19
      4.1.3 Atom optics and laser requirement 19
   4.2 Drag-free AI configuration for self-gravity gradient compensation 20
   4.3 Laser ranging interferometry 21
5. Other possible science measurements and significance 22
6. Summary 23
7. Acknowledgement 25
8. Institution Required Disclaimer 25
9. References 25

1. Introduction

1.1 The most important science question in cosmology

One of the most fundamental challenges in the understanding of physics that governs our cosmos is to explain the observed accelerating expansion of the universe. Space appears to be evenly filled with "dark energy," which makes up nearly 70% of the total mass-energy of the cosmos. This poses a conundrum, because a straightforward argument from quantum field theory suggests that the dark energy density should be tens of orders of magnitude larger than what is observed. The solution to this *cosmological constant problem* clearly lies outside the known realms of gravitational theory. New physics may therefore be needed to provide an explanation. While no entirely successful solution to the cosmological constant problem has been devised yet, it is likely that it will contain light scalar fields that couple to normal matter [1]. These plausibly new and previously unknown scalar fields would have a mass at or below the Hubble scale $H_0 \sim 10^{-33}$ eV (a heavier field would have reached equilibrium and become irrelevant for the current evolution of the universe), and couple to the particles of the standard model with roughly the same strength as gravity (a field that is too weakly coupled would not be able to suppress the large contributions of the standard model vacuum to the cosmological constant).

Any light scalar field that couples to matter with roughly the gravitational strength will lead to new types of force, typically referred as "fifth forces." Their effects, however, must be highly suppressed on solar system scales and undetectable with current technology and experiments; otherwise, it would contradict precision tests of General Relativity that have been performed so far. Viable theories of dark energy achieve this suppression by making the interaction between

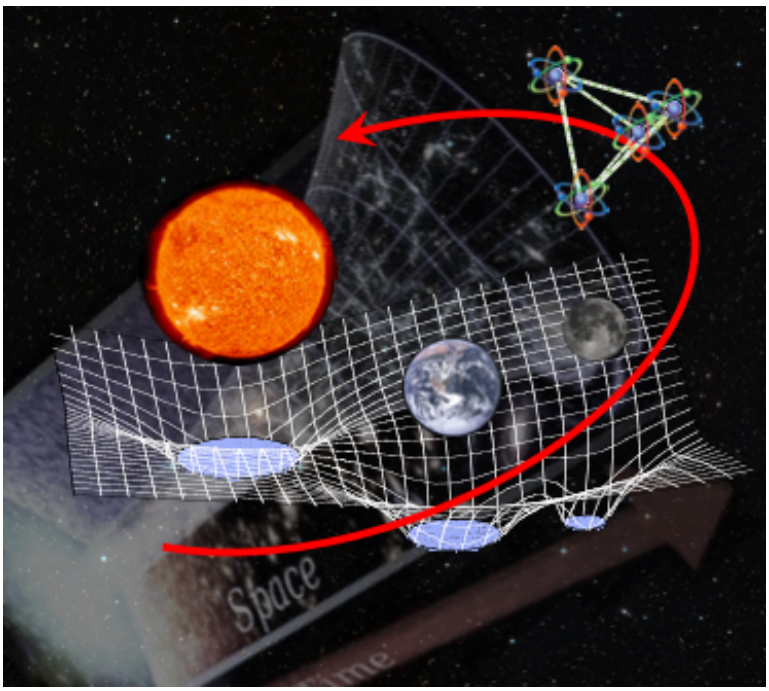

Figure 1. Illustration of the proposed mission concept – a tetrahedral constellation of spacecraft carrying atomic drag-free reference sensors is flying in the Solar system through special regions of interest. Differential force measurements are performed among all pairs of spacecraft to detection non-zero trace value of the local field force gradient tensor. A detection of non-zero trace, and its modulations through space, signifies the existence of new force field of dark energy as a scalar field and shines light on the nature of dark energy.

normal matter and the dark energy fields *environment-dependent*. The mechanism for doing this is called *screening*. Environment-dependent screening works by changing the coupling between matter and dark energy fields in regions of high matter density [2]. A detection of such a coupling in Nature would be a fundamentally new discovery in physics, and would afford us a tremendous opportunity to study dark energy and the cosmos.

There are two general categories of screening mechanisms: the one that depends on local mass densities and another that does not. In the scalar field theories that depend on the local mass densities, such as chameleon and symmetron [2], only an outer thin layer of an extended object will source and interact with the dark energy fields. This is known as the thin shell effect. Since only a thin shell of an object will experience the dark energy force, the overall observable effect of dark energy is thus reduced so that interactions are only dominated by the gravitational force. The short-range force can be in principle detected and verified by precision laboratory experiment measurements. When applying to microscopic objects such as atoms, the depth of the thin shell is larger than the radius of the atoms, leading to partial unscreening. This property, together with isolating an enclosed region from the external environment due to the thin shell effect, has been recently exploited to extend the exclusion regions in the parameter spaces for both thin-shell models by orders of magnitude [3] [4] [5] [6] [7]. Beyond terrestrial laboratory experiments, similar experiments conducted in microgravity environments in space are expected to improve the tests drastically and give more definitive conclusions about the thin shell models [3].

The other type of screening mechanism, the Vainshtein screening mechanism, is completely different [8]. The equation of motion of the Vainshtein scalar field, mediated by a "galileon" field, is highly nonlinear, and the strength of nonlinearity is parameterized by a coupling constant r_c. The screening boils down to the galileon force that falls off like gravity ($1/r^2$) very far away from matter (beyond a Vainshtein radius on the order of 100's of parsecs) but much slower ($1/\sqrt{r}$ for cubic galileon) when getting close to matter. The vast scale of the Vainshtein radius *precludes any possible physical ground laboratory tests of this type of scalar field*. Current experimental constraints on r_c are bounded only by the tests of the inverse square law of gravity using lunar laser ranging and the propagation of gravitational waves [8] [9] [10]. In a cosmological context, on the other hand, the galileon itself is theoretically better motivated as an explanation for the dark energy field.

In this NIAC study, we embrace the challenge of direct detection of the galileon dark energy field in the Vainshtein model. We developed a mission concept to *directly* measure the galileon field using the solar system as a laboratory. The experiment scheme involves precise measurements of the trace of the total scalar force gradient tensor. A tetrahedral constellation of four spacecraft measures the "local" traces while orbiting about 1 AU away from the Sun and far away from planets (Figure 1). The trace measurement is insensitive to the much stronger gravity field which satisfies the inverse square law and thus is traceless. Atomic test masses and atom interferometer measurement techniques are used as precise drag-free inertial references while laser ranging interferometers are employed to connect among atom interferometer pairs in spacecraft for the differential gradient force measurements. We conclude that such a mission is scientifically and technologically feasible. We show that a mission of 3-year measurement time would be able to provide high confidence statements (over 3 standard deviations) about the existence and strength of the cubic galileon field of the Sun. In addition, such a mission would also provide rich and diverse scientific data for testing any gravitational theory in general beyond the Newtonian gravity, hunting for ultra-light fields of dark matter, and detecting gravitational waves in the mid-frequency

band between those of LIGO and LISA. For these reasons, we will term the mission concept Gravity Observation and Dark energy Detection Explorer in the Solar System (GODDESS).

1.2 Challenges in direct detection of dark energy scalar fields

Gravity as described by Einstein's theory of general relativity has been subject to the most stringent tests through both solar system observations and laboratory experiments, and to date without any indication of a violation. To be consistent with the observations so far, any dark energy scalar field model must necessarily have a screening mechanism. The force predicted by dark energy scalar field theories must be weak on non-cosmological scales such as the solar system. Based on current well-motivated dark energy field models, the estimated dark energy force is ten orders of magnitude (10^{10}) weaker than gravity [8]. On the other hand, the gravitational force strength, as determined by the gravitational constant G, is only known to 5 decimal places. Therefore, a direct detection of dark energy will not only require force measurement sensors beyond the current state of the art, but also demand the ability to address the presence and interference of the ubiquitous and much stronger gravitational force. To have a chance of successful detection of dark energy, we must have novel and more sensitive force measurement schemes, measurement strategies to differentiate the weak dark energy force from that of the purely gravitational forces, as well as a reasonable understanding of screening mechanisms and how the dark energy field is influenced by the presence of matter.

This leads to the focus of our NIAC study – *development of a mission concept with strong suppression of gravity effects through the deployment of the new and enabling atom interferometer force sensors*. We explored differential measurement configurations to suppress gravity effects while maintain the expected dark energy signals. The mission concept has been analyzed both for its science and engineering feasibilities. At the same time, currently outside the NIAC effort and through internal JPL funding, we have initiated an effort to accelerate our understanding of how the Vainshtein field is screened by the presence of solar system celestial bodies and where one should look for the dark energy force. The results of this study will guide us in the overall mission concept design by determining the optimal orbits of spacecraft and measurement configurations.

1.3 Innovative approaches and significance

In the study, we investigated the measurement concept using new sensor technologies and innovative methods to tackle the challenges. The first key innovation is in the deployment of atom interferometry (AI), a new weak force measurement technology based on laser cooled ultra-cold atoms. It has been successfully demonstrated in research laboratories and is being commercialized in industry for certain terrestrial gravity measurement applications. We propose to extend the use of cold atom interferometers to operate in the open space environment, that is, atomic test mass particles are freely floating in space outside spacecraft, rather than in an enclosed vacuum chamber, to (a) maximally exploit the sensitivity of AI in microgravity environments, and (b) mitigate spacecraft self-gravity gradient forces.

Atom interferometry exploits the quantum wave nature of atomic particles. Light-pulse atom optics are used to split and recombine atom waves and form the matter wave interferometers. The sensitivity of atom interferometers to inertia forces is determined by the effective lengths of the interferometer arms. To reach an unprecedented measurement sensitivity necessary for dark energy detection, the arm length of the atom interferometers need to extend beyond the any reasonable vacuum enclosure size on a spacecraft. Having atoms in open space removes such

limitations and the corresponding limit of achievable sensitivities. This enables the increase of the instrument measurement sensitivity necessary for direct detection of galileons in the solar system.

With the required extreme force sensing sensitivity comes equally demanding systematic control. One of the biggest challenges of reducing measurement systematics is addressing the spacecraft mass self-gradient forces. This requirement has been highlighted by the stringent spacecraft drag-free requirements in the LISA mission for gravitational wave detection. With ultra-cold atoms as test masses that can be identically reproduced and replaced, drag-free measurements can be achieved without flying spacecraft drag-free. By placing atomic test masses away from the spacecraft masses rather than at the center of mass (CM) of the spacecraft, and by well-designed local differential measurements, we can lower the self-gravity gradient and therefore eliminate self-gradient forces as the dominant error source.

The second key innovation is in the concept of the measurement scheme for suppression of gravity force interference by utilizing the unique property of non-Newtonian gravitational forces. Newtonian gravity, as governed by the inverse square law, has *strictly universal* zero trace of the field gradient tensor in space away from any mass source. Any deviation from the inverse square law behavior, as would be expected from the dark energy force, would exhibit a non-zero trace value, an indication of the existence of the dark energy force. This is the key to realizing high suppression of gravity-induced systematic effects and thus facilitating model-independent discrimination of the dark energy signature in the proposed mission concept. The method is very powerful. It makes the measurements of weak unknown forces possible in principle without the need of precise knowledge of the gravitational force strengths. At the same time, it makes the scheme more practical as the trace value is independent of the measurement orientation relative to mass distributions. This lessens the requirements for the spacecraft constellation control and orbit trajectories. Indeed, by designing the measurement constellation to be tetrahedral and performing simultaneous differential measurements in each of the six arms, the local trace of the force field gradient tensor can be determined regardless of the orientation of the constellation relative to the solar system and its planets.

2. Enabling Technology – Atom Interferometry

2.1 Laser cooling and light pulse atom interferometer

Laser cooling, trapping, and manipulation of atoms are at the heart of the atomic sensor that exploits atomic quantum properties of wave nature. Cold clouds of millionth of a degree above absolute zero temperature can be generated in less than 1 s, and no cryogenic cooling is involved. Atoms at these low temperatures exhibit quantum wave behavior pronouncedly such that each of them is like an extended fuzzy ball rather than a particle in space. The fuzzy balls, or atom-wave packets, can be used to form matter-wave interferometers by using laser pulses as atom optics, similar to optical Mach-Zehnder interferometers formed by several beam-splitters and mirrors. This the atom interferometer scheme, however, the roles of light and matter are reverses. It turns out that the atom interferometers can be very sensitive to small motional changes (accelerations).

The cold atoms can thus be used as test masses in their free fall state. Their acceleration relative to the instrument platform (spacecraft) is measured through the resulting phase shift in the atom-wave interferometer formed by the atomic test masses themselves. Relying on the intrinsic momentum of photons, light pulses driving atomic transitions (typically Raman transitions) are used to function as the atom optics equivalent of beam splitters and mirrors. As illustrated in Figure 2, a "$\pi/2$" laser pulse at time t_1 first creates an equal superposition of the two hyperfine ground

states of the atoms. The excited state receives a recoil kick of 2 photons, and therefore travels at a slightly different velocity, realizing a beam splitting analogous to the input beam splitter in a traditional Mach-Zehnder interferometer. A "π" laser pulse, on the other hand, completely flips the states and functions as a mirror. Hence, a sequence of π/2-π-π/2 at t_1, $t_2 = t_1$+T, and $t_3 = t_1 + 2T$, respectively, completes an interferometer loop. The final transition probability resulting from this interferometer sequence is given by $P = ½[1 - \cos(\Delta\phi)]$, where $\Delta\phi$ is the net phase difference between the two interferometer paths. It can be shown that $\Delta\phi = \mathbf{k}_{\text{eff}} \cdot \mathbf{a}T^2$, where **a** is the atom's acceleration relative to the platform and $\mathbf{k}_{\text{eff}} \equiv \mathbf{k}_1 - \mathbf{k}_2$ (so that $k_{\text{eff}} \approx 2k_1$) is the effective Raman laser wave number [11] [12]. The transition probability P and therefore the phase $\Delta\phi$ are recorded by measuring the relative populations of the two hyperfine states using laser-induced fluorescence detection.

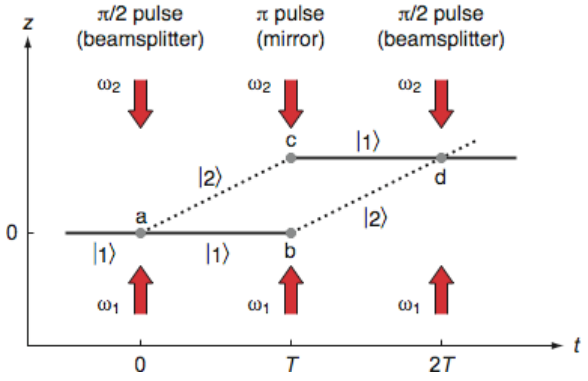

Figure 2. Schematic diagram of the light-pulse atom interferometer. In this scheme, light pulses act as beam splitters (π/2 pulse) and mirror (π pulse) for the atom waves. A phase shift results in the presence of an acceleration.

The sensitivity of the above described atom interferometer (AI) realization can be further increased. Instead of two-photon momenta exchange during the Raman process, an atom can receive more photon momenta ($2n$) that effectively increases $\mathbf{k}_{\text{eff}}$ to $n\ \mathbf{k}_{\text{eff}}$ and thus the sensitivity to the acceleration **a** with the same interrogation time T. The use of more than two-photon transfer for matter wave splitting and recombining is known as large-momentum-transfer (LMT) atom interferometry, and there are variety of means to implement such beam splitters. Methods include high-order Bragg diffractions [13], sequential pulses, spin-dependent kicks, etc. The specific choice of method depends on application-specific tradeoffs, mostly among available laser power, frequency control complexity, requirements on atomic sample temperatures, and systematics.

The attenable acceleration sensitivity per shot of an AI can be quantified by the expression:

$$\delta a = \frac{\delta\phi}{n k_{\text{eff}} T^2}$$

where $\delta\phi$ is the phase resolution of an AI. Fundamentally, for N independent participating atoms, $\delta\phi$ is limited by the quantum projection noise of $1/\sqrt{N}$. For N=10^6, 780 nm AI laser ($\mathbf{k}_{\text{eff}}$ =4π/780nm) for rubidium (Rb) atoms, the acceleration sensitivity is $\delta a = 62/(nT^2)$ pm/s^2, where T is in seconds. Extrapolating to longer T available in microgravity environments in space, AI is extremely sensitive measurement technology for weak forces in space.

Typical AI with cold thermal atoms is realized in an ultra-high vacuum (UHV) cell with a magneto-optical trap (MOT) that forms a potential well for atoms. This trap is made up of a combination of magnetic quadrupole field and three pairs of counter-propagating laser beams (see Figure 3). They are arranged in such a way that atoms are in a viscous light bath (optical molasses) and being constantly pushed toward the center of the trap. With the appropriate detuning of the laser frequencies from the atomic resonance, atoms in the UHV cell can be cooled below 2 μK, corresponding to a root-mean-square (rms) velocity of 1 cm/s for Rb. This low kinetic energy

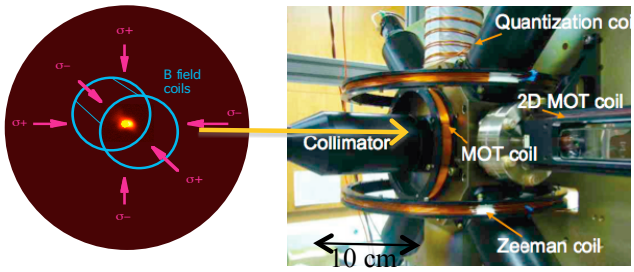

Figure 3. Left: a false color image of an ensemble of cold Cs atoms (yellow) in the middle of a magneto-optical trap that consists of a pair of magnetic coils (blue) and three pairs of counter-propagating laser beams (red); Right: the magneto-optical trap subsystem with the vacuum cell in the JPL transportable gravity gradiometer sensor instrument with the magnetic coils and laser collimators clearly shown.

allows atoms to freely float in space for an extended period of time during which motional changes of atoms can be sensitively measured.

For GODDESS and other demanding space applications, long interrogation T is required. The above mentioned thermal velocity and associated expansion is inadequate. A much colder atomic sample, the Bose-Einstein Condensate (BEC), is necessary to achieve necessary long interrogation time and AI sensitivities. BEC (Nobel Prize in 2001 [14]) is a macroscopic phenomenon of a group of microscopic objects of atoms (Figure 4) [15]. At low temperatures, the wave aspect of atoms becomes dominant so that atoms are like fuzzy balls. When the temperature is low enough, the fuzzy balls of atom inside a trap start to overlap with each other. Due to Bose-Einstein statistics for atoms with integer spins such as ^{87}Rb, they tend to flock into the same state, i.e., to synchronize with each other. The same motional and internal states correspond to lower entropy and thus lower temperature. This positive feedback process of lowering the cloud temperature results in a situation where a significant fraction of the atoms in the cloud is in a single quantum state, the Bose-Einstein Condensate.

In addition to its fascinating quantum state with macroscopic numbers of atoms, BEC is an ideal source for ultra-cold atoms, which is critical for long interrogation time atom interferometers. For instance, a point-like ^{87}Rb cloud will expand to a ball of 6 mm radius in 1 s, if it is at the photon-recoil temperature of 360 nK, the lowest possible temperature achievable without BEC. Extended clouds need even larger laser beams to address, larger vacuum chambers to house, and are more prone to spatial systematic effects in precision metrology. A BEC source can provide clouds of temperatures 10 nK or lower. More recently, well spatially localized atoms in a BEC generator are also subject to the so called delta-kick cooling, leading to effective temperature in the range of pK.

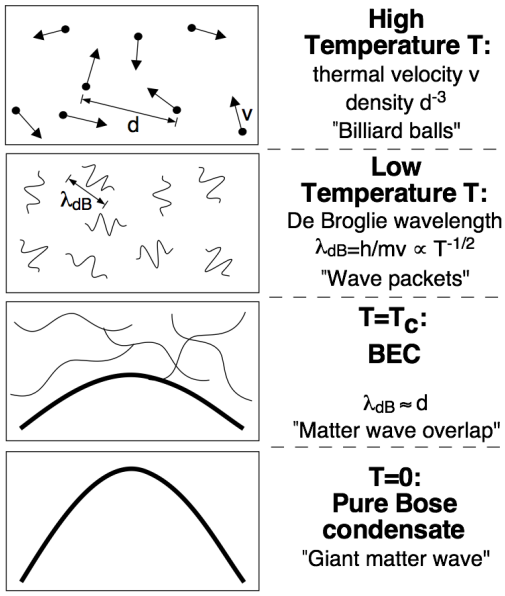

Figure 4. Criterion for BEC [15]. At high temperatures atoms are point-like (top). At lower temperatures atoms are more wave-like and overlap with each other.

2.2 Atomic test mass for the mission concept

In addition to the achievable sensitivities of AI measurements in space, GODDESS requires measurements of relative accelerations between spacecraft for an extended period to distinguish minute effects caused by the Vainshtein field of the Sun. Thus, long-term stable inertial references are critical to the mission's success.

The atom interferometer technology, similar to atomic clocks, is the only technology capable of providing stability over a long time, at the time scales of months, as evidenced in the demonstrated Earth gravity measurements [16]. The AI sensitivity will be much improved due to long T in space, while the property of long-term stability is expected to maintain, i.e., a constant noise spectral density down to very low frequencies close to DC.

By providing stable inertial references, drag-free measurements are implied automatically. Drag-forces include all non-gravitational forces as well as local mass gravity disturbances. Prior to the advent of AI, the only way to achieve drag-free measurements is to fly spacecraft drag-free, as it is the design of LISA spacecraft. In the realization of flying drag-free, a bulk test mass is caged inside a spacecraft at its center of mass and micro thrusters onboard the spacecraft keep the spacecraft body moves as closely to the free fall test mass as possible.

From another viewpoint of flying drag-free, AI is a measurement of relative acceleration between freely falling ultracold atoms and the platform, where the atomic samples are generated anew at the same location on the platform for every measurement. In this picture, atoms serve as an ideal instantaneous inertial reference co-moving with the platform. Refreshing and/or repositioning the atom samples to the exact location of the spacecraft at each measurement means there is no risk of spacecraft eventually running into and colliding with the test mass. And to the extent where the relative motions between the atomic test mass cloud and spacecraft is small during each measurement time, the measurement can be treated as drag-free. This would be the case for Earth gravity missions [17].

On the other hand, GODDESS, similar to LISA, requires exquisite drag-free controls. Whether it is the concept of drag disturbance reduction system in LISA, or that of GODDESS, the required drag-free controls can be only achieved in combination with reducing the shelf-gravity gradient of the spacecraft by carefully arranging the mass distribution. Even thruster fuel consumption over time must be taken into account. Another way to reduce the spacecraft self-gravity disturbances is to move farther way from the mass of spacecraft. Atomic test masses allow us to do that. Indeed, the GODDESS mission concept rely on the ability to operate the atom test masses outside spacecraft where the self-gravity gradients are sufficiently subsides at $1/R^3$ dependence. The GODDESS calls for operating the atomic test masses over 100 m away from the main spacecraft. Furthermore, two symmetrically placed test masses on each side of the spacecraft is envisioned to completely remove the spacecraft drag disturbances.

2.3 State of AI developments for space

The development of AI is very active worldwide. In research labs, the progresses include LMT AI of >100 photon-momentum beam splitters [18], large matter wave-packet separation of single atoms in a 10 m atomic fountain [19], and super-cold atomic samples [20]. Efforts by international space agencies towards space applications include the 100 m drop tower microgravity experiments [21] and the sounding rocket experiments by DLR [22], zero-g parabolic flights and space gradiometer project by CNES [23], atomic interferometric gravitational wave space observatory by US [24] and Chinese space agency [25] respectively, Space-Time Explorer and QUantum Equivalence Principle Space Test (STE-QUEST) led by UK and funded by ESA [26]. NASA has had extensive interests and investments on AI development as well, including Earth science observations by JPL [27] and by Goddard [28] (Instrument Incubator Programs), planetary science (Planetary Instrument Definition and Development Program) [29], and gravitational wave

detection [30] (NIAC). Most significantly, NASA launched the Cold Atom Lab (CAL) developed and operated by JPL [31]. CAL will be the first cold atom research facility in an orbiting space and it includes the atom interferometer experiments and technology demonstrations for future space experiments such as GODDESS. These technology maturation demonstrations will lay solid foundations for future dedicate missions that will exploit the full capability of atom interferometry.

3. Measurement Concept and Mission architecture

3.1 Measurement strategy – Tracelessness test for the unknown force

The cubic galileon, which features the Vainshtein screening mechanism, does not have the thin shell effects as in the chameleon and symmetron models. It modifies the Newtonian gravity over long distance! At ranges greater than the Vainshtein radius (~100 pc for the Sun), the galileon field produces a force that satisfies the inverse square law (ISL); at ranges smaller than the Vainshtein radius, however, the force deviates from the ISL as $1/\sqrt{r}$. Thus, a viable direct detection of the galileon force can be implemented as tests of the ISL. The feasibility of such a direct measurement is predicated crucially on the anticipated signal size, achievable instrument sensitivity, and mostly importantly suppression of systematic effects.

For the purpose of estimating the signal size and discussion of the mission concept design, we use the possible galileon signal resulting from the most massive body of the solar system, the Sun. We will also ignore the influences of other planets for the moment, although they can impact local galileon forces and induce modulations throughout the solar system. These changes and modulations can be taken advantage of, to be discussed later. Based on the cosmologically relevant value of the coupling constant $r_c = 6000$ Mpc, the solar galileon acceleration is $\sim 10^{-13}$ m/s^2 at 1 AU (given by the analytic solution of a spherical uniform body of the Vainshtein equation [32]). The corresponding gravitational acceleration at the same distance about is 6×10^{-3} m/s^2. So, the galileon force is extremely week, about 10 orders of magnitudes (10^{10}) weaker than the gravitation force for the solar system celestial bodies, which explains why we have not seen any violation from the Newtonian gravity in the solar system so far. Similarly, the force gradient of the galileon is $\sim 10^{-24}$ /s^2 at 1 AU, while the gravity gradient is 8×10^{-14}/s^2. Figure 5 plots the galileon field gradient strength (solid blue, Laplacian of galileon) as a function of the distance from the Sun in the solar system, while the radial gravity gradient of the Sun (dashed red) is also plotted for comparison.

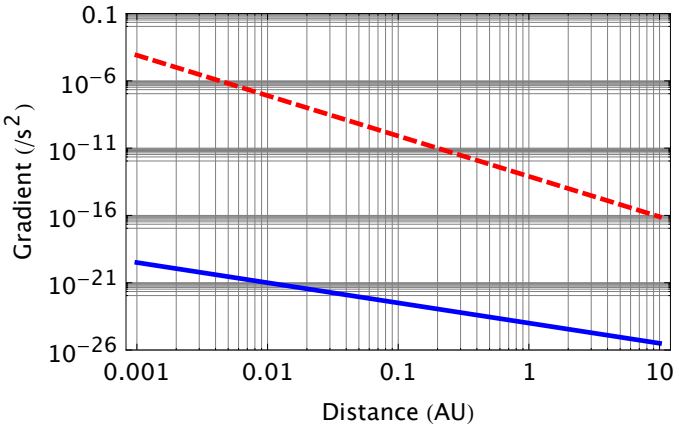

Figure 5. Comparison of galileon signal and gravity gradient of the Sun. Solid blue: Laplacian of cubic galileon due to the Sun. Dashed red: Radial gravity gradient of the Sun.

It is important to realize that the difficulty is not simply because of the weak strength of the galileon force compared to that of gravity. Typical approaches of precision metrology for gravity

exploration include measurements of acceleration, or differential acceleration (gradient). Even with a dedicate instrument having sufficient sensitivity for the galileon, the lack of knowledge of the mass of the Sun (or the $GM_\odot$ product, known to 7×10^{-11} [33]) and of the pointing and the distance to the Sun make it impossible for a detection of the minute galileon signal out of the overwhelming gravity signal. One simply cannot overcome the gravity-induced systematics in the measurements by brutal force.

Our unique and innovative approach to deal this particular set of challenges is to conduct a precision test of tracelessness of the gravity gradient tensor. It is well-known that the trace of the gravity gradient tensor $\overleftrightarrow{\gamma}$, being a 3x3 matrix, in vacuum is invariantly zero:

$$\overleftrightarrow{\gamma} = \begin{pmatrix} \gamma_{11} & \gamma_{12} & \gamma_{13} \\ \gamma_{21} & \gamma_{22} & \gamma_{23} \\ \gamma_{31} & \gamma_{32} & \gamma_{33} \end{pmatrix}, \gamma_{11} + \gamma_{22} + \gamma_{33} = 0.$$

This property is unique to all $1/r$ potentials, whose forces satisfy the ISL and Laplacians are zero in source-less regions. Since the Laplacian is linear, it is independent of the source distribution. On the other hand, the galileon force, with $1/\sqrt{r}$ dependence, will induce a non-zero trace, of the same amplitude as the force gradient. (Radial gradient of a spherical $r^{1/2}$ potential is $\frac{\partial^2}{\partial r^2} r^{1/2} = -\frac{1}{4} r^{-3/2}$, while the Laplacian is $\frac{1}{r^2}\frac{\partial}{\partial r}\left(r^2 \frac{\partial}{\partial r} r^{1/2}\right) = \frac{3}{4} r^{-3/2}$.) A direct measurement of the trace of the local gradient tensor will therefore strategically bypass all the nuisances of the gravitational effects, allowing access to galileon signal without the precise knowledge of the mass distribution or the gravitational constant G. Additionally, the trace of a symmetric tensor is rotational invariant, which means that the specific orientation of the measurement instrument is not critical and that the performance of star trackers for spacecraft pointing poses no severe limitation on the performance of the instrument.

It should be recognized that there are locations where gravitational forces or gradients balance out between celestial bodies such as Lagrange points. The exact positions, directions, and their tolerances again are tied to the GM products. There are regions of interests as the gravitational force or gradient strengths are greatly reduced, though at this point, it is not clear how corresponding galileon forces show up in these special points.

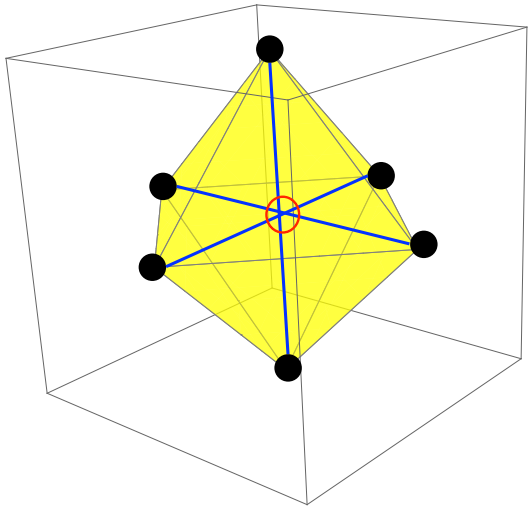

Figure 6. Illustration of three orthogonal gravity gradiometers. Gravity gradients are measured between each pair of spacecraft (block dots) along three directions (blue segments). Trace of gravity gradient tensor at the center location (red circle) can then be inferred.

3.2 Robust measurement configuration

To measure the trace of the gradient tensor, a straightforward arrangement is to have three orthogonal gravity gradiometers formed by a spacecraft constellation to measure the three diagonal elements of the force gradient elements of the matrix (Figure 6). The sum of the three diagonal elements gives the trace. Given the required precision needed for the non-zero galileon signal, each

gradient measurement must be accurate to one part per 10^{10} in order to guarantee the sum gives the residual at 10^{-10} precision. This requires high precision on orthogonality and on overlap of the mid points of all gradiometers, which would in term requires specific formation of the spacecraft relative to the solar bodies and thus sophisticated control thrusters and spacecraft trajectories. For instance, consider a measurement at 1 AU where the diagonal elements of the gravity gradient tensor of the Sun are $\sim 10^{-14}$ /s^2. In the configuration where the three-axis gradiometers are oriented along the field principal axes, a misalignment of 10^{-10} rad would induce proportionally of 10^{-24} /s^2 in one axis while quadratically in another of negligible magnitude. Thus, the induced overall trace measurement error will be comparable to that of the expected galileon signal. With the current star-tracker technology or laser ranging schemes, a spacecraft formation of 10^{-10} rad alignment precision is nearly impossible.

A much more robust measurement configuration would be having the all spacecraft in the constellation follow their natural trajectories and the measurements insensitive to the changes and the orientation of the constellation. Such a configuration is indeed possible with a regular tetrahedron formation in space, as depicted in Figure 7. With the differential accelerations measured in the six directions along the lines connecting the pairs of spacecraft, the gradient tensor, being a symmetric 3x3 matrix, can be uniquely determined and the trace of it can then be measured. In this configuration, only the relative angles of the lines of measurements are critical, though still as stringent. But the angles can be precisely determined if the distances between spacecraft are precisely measured. This can be accomplished in principle by high-precision laser ranging and tracking. Note again that the overall orientation and the exact shape of the constellation are dynamic, the elements of the tensor are changing accordingly, it will not affect the trace and thus the detection of the unknown forces.

Overall, the measurement scheme requires three major ingredients: laser ranging, inertial reference, and the systematics in trace determination. In the following sections, each aspect will be discussed in more detail.

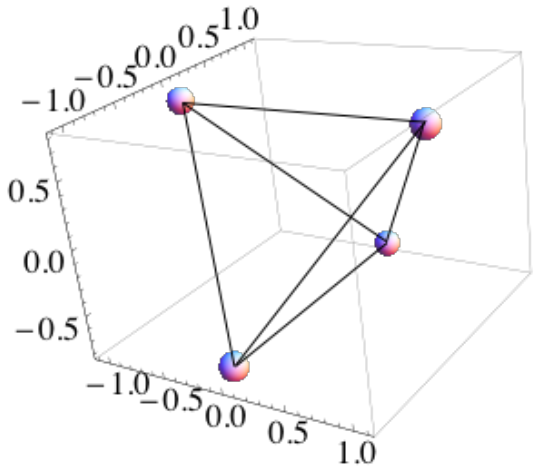

Figure 7. Concept for gradient tensor measurements. Spacecraft (spheres) form a tetrahedron, and the distances are measured by laser ranging (black lines). Along the laser ranging directions, precise relative accelerations are measured. The gradient tensor can then be obtained via the six gradient measurements.

3.3 Measurement of gradient tensor and trace

In the configuration depicted in Figure 7, the gradient tensor $\overleftrightarrow{\gamma}$ can be determined through measurements of field gradient along six non-parallel directions as follows. The field gradient $\tilde{\gamma}_{ij}$ along the direction $\hat{L}_{ij} = (l_\xi, l_v, l_v)$ of spacecraft i, j is determined by the differential acceleration δa_{ij} divided by the armlength L_{ij} (see Ref. [17] and to be detailed in Section 3.5): $\tilde{\gamma}_{ij} = \delta a_{ij}/L_{ij}$. $\tilde{\gamma}_{ij}$ relates to the gradient tensor $\overleftrightarrow{\gamma}$ as $\tilde{\gamma}_{ij} = \hat{L}_{ij} \cdot \overleftrightarrow{\gamma} \cdot \hat{L}_{ij} = \sum_{\alpha\beta} l_\alpha l_\beta \gamma_{\alpha\beta}$. Thus, with six measurements $(\tilde{\gamma}_{ab}, \tilde{\gamma}_{ac}, \tilde{\gamma}_{ad}, \tilde{\gamma}_{bc}, \tilde{\gamma}_{bd}, \tilde{\gamma}_{cd})$ between spacecraft a, b, c, d, and the point vectors $\hat{L}_{ij}$ obtained from the triangulation of the spacecraft constellation, $\overleftrightarrow{\gamma}$ that has six degrees of freedom

$(\gamma_{11}, \gamma_{12}, \gamma_{13}, \gamma_{22}, \gamma_{23}, \gamma_{33})$ can be calculated uniquely in the reference frame, which does not have to be along the principal axes of $\overleftrightarrow{\gamma}$. Mathematically, it is a process of solving the following linear equations

$$\begin{bmatrix} \tilde{\gamma}_{ab} \\ \vdots \\ \tilde{\gamma}_{cd} \end{bmatrix} = [l_\alpha l_\beta] \begin{bmatrix} \gamma_{11} \\ \vdots \\ \gamma_{33} \end{bmatrix},$$

$$\text{thus} \begin{bmatrix} \gamma_{11} \\ \vdots \\ \gamma_{33} \end{bmatrix} = [l_\alpha l_\beta]^{-1} \begin{bmatrix} \tilde{\gamma}_{ab} \\ \vdots \\ \tilde{\gamma}_{cd} \end{bmatrix},$$

where $[l_\alpha l_\beta]$ is a 6x6 matrix solely determined by the orientations of $\hat{L}_{ij}$ in the reference frame.

Although the components determined depend on the reference frame of choice, the trace $\gamma_{11} + \gamma_{22} + \gamma_{33}$ is not. This is the reason why only precise relative angles between $\hat{L}_{ij}$ are critical but not the overall pointing of the constellation for the tracelessness test.

3.4 Drag-free inertial references

The trace value of the force gradient tensor is obtained through the measurements of a set of the force gradient components as described previously. Each gradient component is a differential measurement of the accelerations on the local test masses. Normally, separate measurements are made of each local test mass relative to the spacecraft reference point which are connected through the laser ranging interferometers as discussed in the previous section. In order for the measured force gradients only of that of gravity and the galileon sources, the test masses must be drag-free, that is, there is no non-gravitational forces on the test masses including the local spacecraft self-gravity influences. In additional, the precision, especially the measurement scaling factor must be stable over the entire measurement time, that is, the mission lifetime, as the measurements are aimed to determine a single value of the trace. Nevertheless, possible signal modulations and spatial dependences are being considered to help improve the essentially a very low frequency (practically DC measurements without any spatial modulation.)

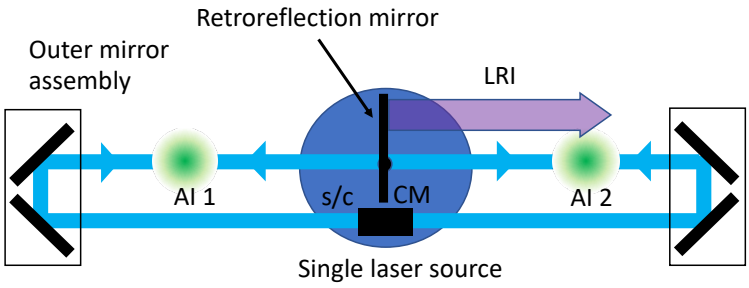

Figure 8. Schematic of an inertial reference system utilizing two AIs. s/c: spacecraft. LRI: laser ranging interferometer, sharing the same mirror assembly as the AI retroreflection mirror. Blue lines: laser pulses for atom manipulation and AIs.

This is where we rely on the stability and accuracy of atomic test masses and atom-interferometers. Conventional spring-mass accelerometers, or their modern cousin the state-of-the-art electrostatic accelerometers, tend to drift beyond 1000 s. Positioning accelerometers in spacecraft is also prone to error, even with the drag-free flight of spacecraft due thermal expansions and occasional fuel burning. In short, mechanical accelerometers fundamentally lack the scaling

factor stability required to the long-term averaging of the trace detection. Ultra-cold atomic test masses and the atom interferometer, as detailed in Section 2, can in principle meet the stability and accuracy requirements. Nevertheless, the implementations are not straightforward and systematics must be addressed.

Using the Mach-Zehnder (MZ) interferometer configuration with large momentum transfer (LMT) beam splitters as an example, reaching the required acceleration sensitivity will require AIs to span a distance of >10 m in microgravity. It obviously cannot easily fit into spacecraft, let alone the requirement for gravitationally uniform region near the CM of the spacecraft. The spacecraft self-gradient force will always be the dominating error.

To mitigate this problem, instead of operating the AI at the CM of the spacecraft, two AIs are performed simultaneous far away from the spacecraft straddling the CM in the front and back, as illustrated in Figure 8. Despite the mass distribution of a spacecraft, its potential is approaching that of a point source at large distances, whose force is anti-symmetric about the CM (Figure 9). Using a common retroreflection mirror nominally at the CM, two AIs are operated symmetrically in opposite directions. This can be accomplished by using a common laser source to move atomic clouds from the spacecraft into free space on both sides, and to perform atom-wave splitting and recombining functions for the atom interferometer measurements. The distances of the AIs to the retroreflection mirror will then be identical. The mean acceleration of the AIs is then the relative acceleration of the retroreflection mirror to the inertial frame defined half-way between the two AIs, without any drag influence.

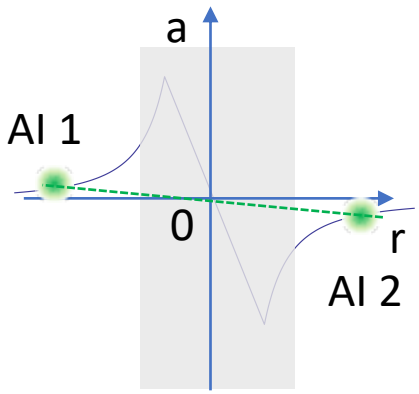

Figure 9. Illustration of extended inertial reference system using AIs. Acceleration (a) versus distance (r) from a spacecraft is plotted. The gray region indicates acceleration deviation from $1/r^2$ due to non-uniform mass distribution of the spacecraft. The average of AI measurements outside the gray region then indicates the acceleration of the retroreflection mirror relative to an inertial frame.

3.5 Laser interferometer ranging

With the spacecraft local drag-free references established as described in the previous section, the gradient forces over a large distance measurement can be considered as a giant (long baseline) gravity gradiometer implementation. In a typical AI based gradiometer implementation, the measurement is done with as much common mode as possible in which a common AI laser is used for interacting with both atom test mass ensembles. This becomes difficult when the separate is large as in this mission concept. It turns out that one can use a laser interferometer ranging technique to connect the two AI lasers or reference points [17] [34], making it effectively a single long baseline gradiometer for the differential measurements.

The laser ranging plays a number of critical roles in the trace measurement concept. First, the laser ranging interferometer (LRI) between each pair of spacecraft is used to track the relative accelerations as the rate of change of Doppler shifts between the spacecraft. Together with the drag-free test masses as the inertial reference points, they determine the inertial force gradient due to gravity and any unknown inertial forces, as illustrated in Figure 10. This is similar to the

gravitational wave detection arrangements in LISA mission. There is a very distinct difference between the force gradient trace measurements in this concept and the LISA gravitational wave detection. In the latter case, the measurement system seeks time varying signals over a set of frequency band, that is 10 mHz to 0.1 mHz [35] at an acceleration sensitivity of about $1x10^{-14}$ $m/s^2/Hz^{1/2}$. For the trace measurement determination, we plan to average the single measurement value down to DC value, that is, as long as the mission takes. The overall acceleration measurement sensitivity is, however, depends on the length of the measurement baseline, that is, the distance between pairs of spacecraft.

The second function of the laser ranging interferometer is to perform actual absolute distance measurements. Indeed, this is necessary for two reasons. Recall that each gradient measurement must have ten (10) digits precision (at 1 AU as an example before). Since the gradient value is determined by the differential acceleration measurement divided by the baseline length, that is, $(\vec{a}_1 - \vec{a}_2)/L$, the baseline must be also determined to the same precision, that is, 1 part per 10^{10}.

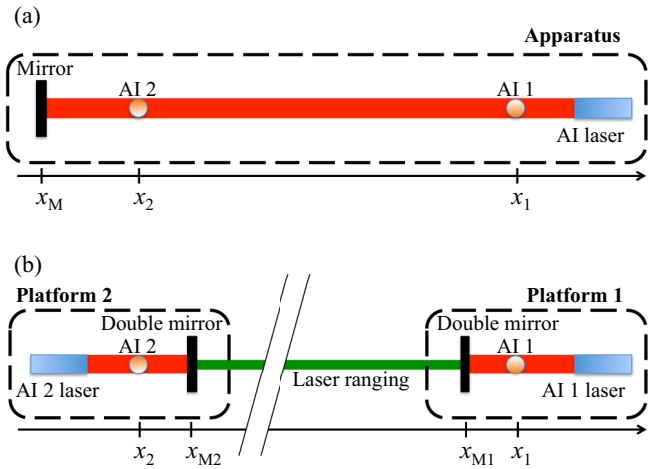

Figure 10. LRI-AI concept. (a)Conventional differential AIs hosted in one apparatus. x_i is the position of the corresponding element. The instrument baseline $L = x_1 - x_2$. (b) Twin AIs linked with a laser- ranging interferometer (LRI-AI). The double mirror has a reflective surface serving as the retroreflection mirror for the AI on one side and serving as the retroreflection mirror for the LRI on the other side [14].

In addition, in order to determine the trace from the tetrahedron configuration measurements, the geometric angles among all measurement directions must be equally precisely determined. We will determine the angles by the precise measurements of all lengths of sides of the tetrahedron [17]. It is not difficult to show that the requirement in terms of the relative length precision is similar to that required by the baseline precision for the gradient measurement itself.

For the baseline of 10^6 m in GODDESS, the uncertainty in ranging has to be better than 100 μm for the gradiometer baselines and for relative angle calculations. For the gravity gradient signal of $\sim 10^{-14}$ /s^2 at 1 AU, the differential gravity acceleration is $\sim 10^{-8}$ m/s^2 with the above baseline. Accordingly, the target galileon signal would be on the order of $<10^{-18}$ m/s^2. Assuming a reasonable 3 year total measurement time in the entire mission duration, the required acceleration measurement sensitivity would be at the level of $1x10^{-14}$ $m/s^2/Hz^{1/2}$, similar to what LISA plans to achieve.

3.6 Choice of baseline length

With a given fractional precision requirement, it is apparent then that it will be advantageous by extending the baseline length as long as possible. In practice, the baseline length cannot be

arbitrarily long. Propagation delay due to long baselines will impose stronger frequency noise requirements for the ranging laser. Additionally, other systematic effects such as higher order gravity field curvature will dominate. There will be tradeoff and optimization to be made.

Gradient is in principle the property of a single spatial point. In practice, it is measured over some finite distance. Since the gradients will be measured over long baselines for achieving the overall measurement sensitivity and precision, the measured value will be the average close to the middle of the baseline. These middle points won't necessarily coincide at a single spatial point with the formation depicted in Figure 7 if all spacecraft are in their own trajectories. Disregarding these displacements will lead to significant error in trace calculation due to non-vanishing higher order derivatives of the gravitational potential. For example, consider a set of gradient measurements at 1 AU using 10^6 m baselines in the tetrahedral formation and the Sun as the sole source. Depending on the orientation of the formation with respect to the Sun, the difference of gradients from the effective locations to the center of the formation varies and is introduced into the calculated trace, as shown in Figure 11 where no instrument noise is assumed. Reducing such an effect to below required sensitivity of 10^{-24} /s^2 by orienting the formation at specific angles, such as 0 and 90 degrees, would require pointing accuracy of the formation to better than 1 mrad in both the polar angle and the azimuthal angle in best cases. Pointing fluctuations will also manifest as noises. Angles that minimize the offset and that minimize the angular sensitivity unfortunately do not coincide.

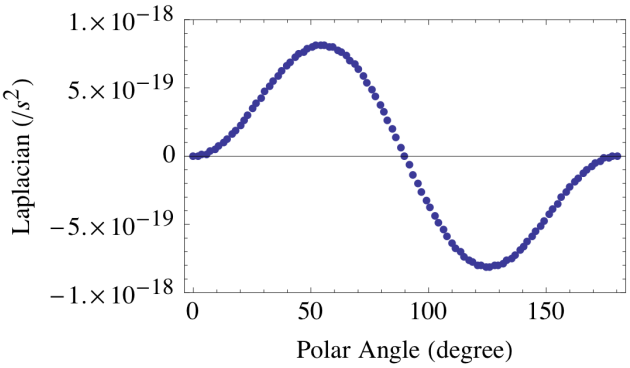

Figure 11. Impact of overlap error. Plotted is the trace of inverted gradient tensor versus the pointing of the spacecraft formation.

This systematic error can be mitigated to some extent by performing the measurements far enough away from the mass source so that the higher order terms become negligible and the systematic error is equal or below the measurement noises. The systematic error here scales as the ratio of the baseline L to the distance R to the Sun, and is proportional to the strength of the gravity gradient $\sim R^{-3}$, resulting in an overall scaling dependence of $\sim LR^{-4}$. On the other hand, for a given acceleration measurement noise, the gradient measurement noise scales $\sim L^{-1}$. For an optimized arrangement, we choose the baseline length L such that the gradient measurement noise is equal to the systematic error described above. In doing so, the optimized length L scales with R^2 and the noise goes as $\sim R^{-2}$. Recall that the galileon signal size scales as $\sim R^{-3/2}$, the resulting signal to noise ratio (SNR) would then scale as $\sim R^{1/2}$. Clearly, one benefits by going out farther away from the main mass source. Figure 12 shows an example of the expected SNR versus R in which

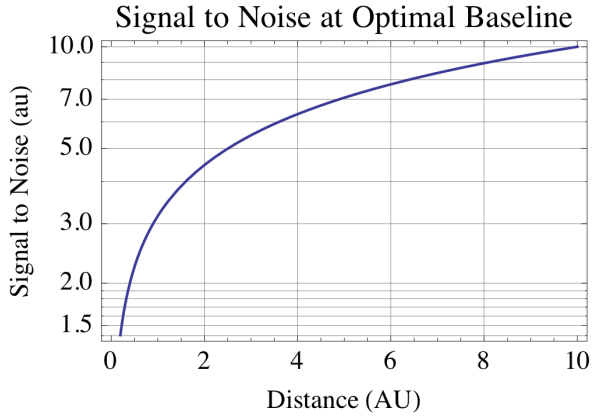

Figure 12. Signal to noise ratio of galileon trace measurement versus distance to the Sun.

10^{-19} m/s^2 differential acceleration noise is assumed. Note that an SNR of 3 can be reached at 1 AU, with which a high-confidence statement of the existence of galileon can be made. Also note that the baseline is chosen to match the systematic error at different *R*, so it varies for the plotted points. The SNR will be further improved if the systematic is to be modeled and the instrument sensitivity is to be adjusted to match the modeling uncertainty, as described below.

There is however another approach to mitigate this systematic. In Section 3.2 discussion, the trace calculation from the tetrahedron measurements treats the gravity gradient as a constant over the baseline of the measurements. This needs not to be the case as we know roughly the overall gravity gradient spatial dependence (largely based on the $1/R$ potential.) It is feasible to correct the measured gradients for the separation of the effective locations without knowing the GM product accurately. This approach is based on a detailed analysis of the gradient measurement and taking into account the higher order derivatives of the $1/R$ potential. The displacement of the effective measurement location and the CM of the formation results in a fractional change of the measured gradient. The fraction depends on relative orientation of the measurement direction to *R*, and the relative length of the displacement to *R*. It can be shown that the differential acceleration in the line of sight direction $\widehat{\delta r_d}$ between two points $\vec{R} + \delta\vec{r}_c \pm \delta\vec{r}_d$ over the separation $2\delta r_d$ (Figure 14), which is regarded as the measured gradient γ_m, is related to the gradient γ_0 at $\vec{R}$ along the same direction $\widehat{\delta r_d}$:

$$\gamma_0 = \gamma_m \left[1 + \frac{\delta\alpha^2}{2}\left(\frac{3 - 30\alpha^2 + 35\alpha^4}{3\alpha^2 - 1}\right) + \frac{3\beta\delta\beta}{3\alpha^2 - 1}\left(1 - 5\alpha^2 - \frac{5}{2}\delta\alpha^2(1 - 14\alpha^2 + 21\alpha^4)\right) + \frac{3\delta\beta^2}{2(3\alpha^2 - 1)}\Big(1 - 5\beta^2 + 5\alpha^2(7\beta^2 - 1) + \frac{5}{2}\delta\alpha^2\left(7\beta^2 - 1 + 7\alpha^2\big(2 - 18\beta^2 + 3\alpha^2(11\beta^2 - 1)\big)\right)\Big) + \cdots\right]^{-1},$$

where $\alpha = \widehat{\delta r_d} \cdot \hat{R}, \delta\alpha = \delta r_d/R, \beta = \widehat{\delta r_c} \cdot \hat{R}$, and $\delta\beta = \delta r_c/R$. The calculation assumes a $1/R$ potential and thus $\gamma_0 = (3\alpha^2 - 1)GM/R^3$. By applying this correction coefficient to simulated gradient measurements and then performing inversion for gradient tensor, the systematic is greatly reduced. Figure 13 shows the result for 10 times longer baseline than that used in Figure 11. The blue points are traces for the solar gravitational potential. Clearly the systematic error is greatly reduced even with much longer baseline. To verify that a non-vanishing trace of other potential type, such as galileon, will not get suppressed by the correction coefficient, a Yukawa potential with $\alpha = 10^{-10}, \lambda = 10^{11}$ m is used for the simulation, which would have a trace of 2×10^{-24} /s^2 at 1 AU, similar to what we expect from galileon. The result is shown in red in Figure 13, which confirms that the correction coefficient will preserve the non-vanishing trace of the gradient tensor. Note that for locations where multiple celestial bodies having comparable gravitational accelerations, the above treatment will need to be modified. This gradient correction scheme will allow measurements much closer to the Sun, where the galileon signal is stronger. Comparing with the results shown in Figure 12, clearly, there still exist trade studies to be made with more detailed mission assumptions and requirements.

3.7 Choice of mission trajectories

There may exist a Goldilocks zone in the Solar system for the galileon detection. The galileon gradient signal scales as $\sim R^{-3/2}$ favoring short distances to the Sun, while the its ratio to the gravity signal increases as $\sim R^{3/2}$ favoring long distances. As suggested in the previous section, the optimal distance depends on the instrument sensitivity and the uncertainty of systematics. Without the correction coefficient for the systematic, the systematic decreases as distance increases, which permits longer baseline to increase instrument sensitivity. The SNR thus increases with the distance to the Sun, until other effects not considered here become appreciable, such as difficulty in establishing LRI with extremely long baseline, time delay noise, topological general relativity effects, and mission costs. In situations where the correction coefficient method applies, the systematic is largely removed, getting as close to the Sun as technically feasible is preferred. Issues that may prevent very small R include extreme solar radiation heating, collisions of cold atoms with particles in solar winds, influences of inner planets significantly altering the $1/R$ potential assumption.

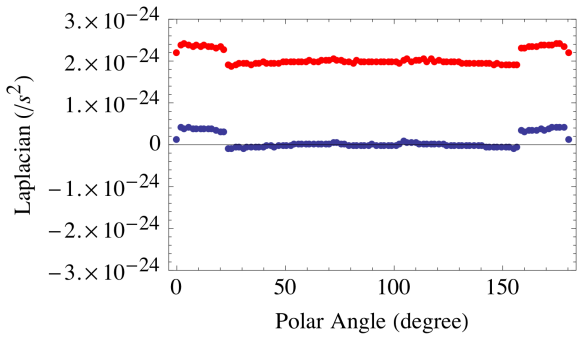

Figure 13. Trace vs formation angle after applying the correction coefficient. Blue: gravitational potential. Red: Yukawa potential. The discontinuities may due to numerical rounding errors.

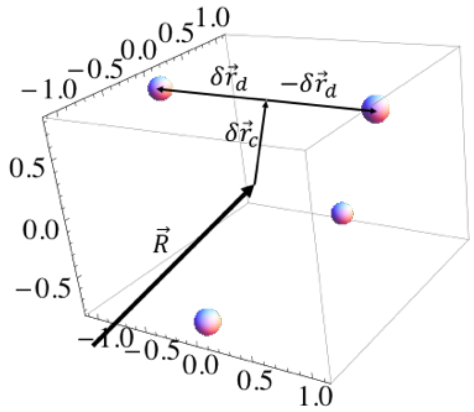

Figure 14. Illustration of gradient correction. The two reference points have common (differential) displacement $\delta\vec{r}_c$ ($\delta\vec{r}_d$) from $\vec{R}$, where the desired measurement location of gradient is.

It is thus desirable to operate such a mission out of the ecliptic plane of the solar system, where the assumptions of single source mass (the Sun) and $1/R$ potential in above calculations are more adequate. Moreover, it is not clear how the galileon field would look like with multiple source bodies, due to the high nonlinearity of the equation of motion, though a numerical simulation effort has been initiated by our team, funded by an JPL internal study, to have a jump start on this important science question but has huge impact to the mission design. At the moment, a natural choice of the trajectory is then a 1 AU near circular orbit out of the ecliptic plane.

It may be advantageous, however, to consider regions with multiple sources when we have a better understanding of how the galileon field manifests itself. For example, in regions where the gravitational gradients of two sources are comparable, the Laplacian of individual sole-source galileon field is also comparable. The nonlinearity of galileon may reduce the Laplacian of the total field to near zero or could increase it significantly, but it is very unlikely that the Laplacian will remain unchanged. Consider a mission that cruises periodically between regions where one body dominates the gravitational force and where two bodies contribute equally, while maintaining similar distance to one body. The Laplacian of galileon will then get modulated by the closeness

of the second body, and thus a modulated signal will be established. For example, assuming that the Laplacians of galileon fields from two sources add linearly, the trace would be twice larger near Lagrange points in the Sun-Earth system than other places 1 AU away from the Sun. Thus, a periodic visit of Lagrange points will periodically increase the signal by 100%.

If the systematic remains proportional to the signal or even stays constant, the SNR will be improved with the signal doubling. More importantly, signal modulation will translate a near DC signal measurements to a higher frequency, which will greatly relax requirements on many systematics including the required intrinsic measurement stability, the spacecraft self-gravity gradient, and effective location displacement.

The orbit of natural choice, 1 AU orbit out of the ecliptic plane, may support this multiple source scenario. The mission can be arranged to fly-by the Earth-Moon system twice a year, so that the modulation can be exploited. Faster modulation may be possible by flying by Mercury rather than the Earth, or other in-plane orbits involving Lagrange points. The choice of the mission trajectories remains largely unexplored and should be in the follow-on study efforts.

4. Technology Feasibilities

The instrument sensitivity of the measurement concept described above relies on two constituents, the laser ranging interferometry and the atomic inertial reference system. In the following sections the state-of-the-art of each of them and the feasibility of supporting a successful mission of direct dark energy detection in the near future will be discussed. All discussions will be based on a measurement with a gradient sensitivity of 10^{-24} /s^2 in 3 years, corresponding to the anticipated galileon signal at 1 AU.

4.1 Atomic inertial reference instrument

Atom interferometers will serve as the local inertial references for LRI. As discussed earlier, to mitigate self-gravity gradient effects of spacecraft, four atom interferometers are employed along each direction of the differential measurement. These AIs will be operated *outside* the spacecraft in free space vacuum. The requirements on AI sensitivity, atom sources, atom optics, and the aspect of free space operation will be discussed in the following subsections. ^{87}Rb is used for the discussion as an example.

4.1.1 AI sensitivity

A Mach-Zehnder AI with large momentum transfer beam splitters of $2n\hbar k$ and an interrogation time T has a maximum per shot acceleration sensitivity of $\delta a = \left(2nkT^2C\sqrt{N}\right)^{-1}$ when the output is residing on a zero crossing of the fringe, where C is the fringe contrast and N is the number of participating atoms. A differential measurement between two such AIs will yield a sensitivity of $\left(nkT^2C\sqrt{2N}\right)^{-1}$ after taking into account of the quadrature addition of uncorrelated noises. For a common measurement, as discussed in the previous sections where AI outputs are added to suppress the self-gravity gradients, the signal actually doubles in the addition process and thus the sensitivity to the mean becomes $\left(2nkT^2C\sqrt{2N}\right)^{-1}$. Assume a contrast of C=0.5, interrogation time of T=10 s, one would need n=200 and N=10^8 (resulting in a 10 m separation between two arms of the AI) or other combinations such that $n\sqrt{N} \geq 2 \times 10^6$. These parameters are in the same range

as those used in the mission concept studies for AI-based gravitational wave detections [34] [24] [36]. While such interferometers are achievable in principle, their realization is challenging as it requires an appropriate space environment for a full demonstration.

4.1.2 Ultra-cold atom source

The temperature of the atom sources is a critical design parameter in the atom interferometer apparatus with the long interrogation times. The atom cloud expansion and dynamics due to the residual kinetical atoms result in spatial dependent effects. Bose-Einstein Condensate of atoms provides a path for reaching ultra-cold pK temperatures, though there is a tradeoff among optimizing cloud temperature and atom number/preparation time/experiment complexity. An adequate atom source should provide a sufficient number of atoms for quantum-projection-noise (QPN) limited AI measurements, while at the same time low enough cloud temperature such that both the degradation of AI fringe quality (fringe contrast) and the associated systematics are acceptable and within the error budget. For simple laser cooled atom sources, $N>10^6$ is quite common with typical temperatures of few μK or few 100 nK and a preparation time of < 1 s. BEC samples of $\sim 10^6$ have also been demonstrated with a typical preparation time of ~10 s.

The thermal expansion rate of a cold atomic cloud is ~10 mm/s at the recoil temperature of ~1 μK, the limit of simple laser cooling. An ultra-cold atom source through BEC usually has temperature ~1 nK, which drastically reduces the expansion rate to ~0.3 mm/s. Consider an AI experiment that requires an interrogation time $2T$ ~20 s, a 1 μK cloud would be 200 mm in radius at the end while an ultra-cold cloud would be only 6 mm. To have a laser beam of Gaussian profile to address the whole cloud with sufficient uniform intensity, the beam size goes quadratic to the cloud size, and the total optical power is quadratic to the beam size!

Thus, to support a direct dark energy detection in space where long AI interrogation times are needed, ultra-cold atoms of pK temperature will be needed. However, a BEC source of $N > 10^8$ has yet to be demonstrated. Current BEC generation schemes utilize evaporative cooling as the final step to reach the condensate state. This step relies on removing hotter atoms in a trap while re-thermalizing remaining atoms, just like a cup of coffee cools due to evaporation. The efficiency of the evaporation is typically on the order of few percent due to high number density and inelastic collisions, and loading atoms into the trap for the evaporative cooling from the initial magneto-optical trap is typically poor as well. Both of which limit the achievable N.

BEC without evaporation, on the other hand, has recently been demonstrated in lab [37]. This alternative approach is promising to significantly increase N and at the same time drastically reduce the preparation time. Work is in progress to pursue high flux BEC generation using this technique. A high-flux fast ultra-cold atom source is a technology gap that needs focused efforts for development and maturation.

4.1.3 Atom optics and laser requirement

The long baseline LRI-AI measurement scheme relies on laser ranging interferometers to extract differential acceleration between distance spacecraft. AI laser beams do not need to travel across the baseline between spacecraft, instead only need to accommodate the travel distance <100 m of the clouds from the source housed on the spacecraft to open space and to accommodate the clouds' thermal expanded size of ~1 cm. Large momentum transfer beam splitters of $\sim 200\hbar k$ can be achieved in the fashion of sequential Bragg diffractions, each of which is $\sim 4\hbar k$. Low order Bragg diffractions require much less optical power than high order ones, while the dynamic phase shifts are also significantly smaller [38]. The AI laser will be stabilized up to 10 GHz detuned from ^{87}Rb

D_2 transitions to suppress the single photon loss, and the beam waist will be up to 10 cm to provide uniform illumination across the cloud. Two frequency components in the laser beam responsible for driving the atomic transition will be generated via an acousto-optic modulator or offset frequency locking. In addition to performing beam splitting in the AI operations, the AI lasers are also used for transporting atomic clouds from the source to open space away from the spacecraft. This will be achieved using moving optical lattices, the Bloch oscillations, established by slowly chirping the frequency difference between the two frequency components. The single-photon loss will be the major concern in this process, since atoms will be exposed in the laser beam for extended period of time for about 1 s. Thus, the detuning will have to be detuned by few hundred GHz.

An estimated total laser power of ~3 W will be required for both the AI and the transport processes. Such a laser system can be realized through the use of optical amplifiers which are available at the Rb wavelengths and as off-the-shelf commercial modules. Frequency generation, modulation, pulse shaping, etc., are well known techniques in laboratory. Space qualification are necessary but do not present any known showstopper.

Operating AIs in total natural space vacuum environment is totally new and has not been demonstrated in any way, though similar approaches were also proposed in the concepts of gravitational wave detection. Since the natural open environment is going beyond typical well controlled lab environment, many environmental effects warrant careful studies. To the first order, typical vacuum requirement for AI experiments is about 10^{-10} torr. This condition can be easily satisfied beyond the medium Earth orbit and away from planetary surfaces. The other major concern should be magnetic field effects though atomic Zeeman shifts. The magnetic environment also had two major components, one from the solar system itself, and one from local sources of spacecraft materials. The former is dependent of the orbits chosen, and the latter the selection and control of spacecraft materials. Similar to reducing the spacecraft self-gravity gradient approach, the self-magnetic gradient is also reduced when the atom clouds are farther away from the sources.

Coherent optical transport using Bloch oscillations has also been demonstrated in laboratory, and can be adapted for this purpose. It however has never been demonstrated to perform AIs in open space vacuum rather than in sealed vacuum chambers. Such a technology demonstration of AIs in open space will be critical for direction dark energy detection.

4.2 Drag-free AI configuration for self-gravity gradient compensation

As discussed in Section 3.4, to realize totally drag-free atomic test mass measurements at the accuracy of the acceleration < 10^{-18} m/s^2, the tolerance of the mid-point of the AIs to the CM needs to be well controlled. Let the acceleration around position *d* outside the gray region in Figure 9 be expanded as $a(x) = a(d + \delta d) = a_0 + \gamma\, \delta d + \cdots + a_G + \gamma_G(d + \delta d) + \cdots$, where $\gamma = 2GM_{sc}/d^3$ is the gravity gradient at position *d* for a point mass M_{sc}, and a_G, γ_G are the acceleration and gradient due to celestial bodies. Symmetric about the CM, the acceleration near position -*d* is $a(-d + \delta d) = -a_0 + \gamma\, \delta d + \cdots + a_G + \gamma_G(-d + \delta d) + \cdots$, since positions ±*d* are far enough away from the spacecraft and that the potential is symmetric about the CM, which by definition has vanishing dipole term in the spherical harmonic expansion. Each AI measures the local acceleration relative to the local acceleration of the retroreflection mirror $a_G + \delta a$. The mean acceleration a_m of the two AIs with mid-point δd offset from the CM is $a_m = -\delta a + (\gamma + \gamma_G)\, \delta d + \cdots$. Without the offset, $\delta d = 0$, $a_m = -\delta a$ indicates the acceleration of the

retroreflection mirror, which will supplement the LRI for long distance gradient measurements between virtual inertial test particles. The error due to the offset and the self-gravity $\gamma\ \delta d$ then need to be below required acceleration resolution, while the virtual inertial test particle will reside δd away from the CM with gravitational acceleration $a_G + \gamma_G \delta d$. Assuming a spacecraft of 500 kg and an offset of $\delta d \simeq 1$ mm, $a_m < 10^{-18}$ m/s^2 requires $\gamma < 10^{-15}$ /s^2, which happens at d > 400 m for an adequate approximation of a point mass potential.

Approaches to further relax the self-gravity gradient requirement without needing access to distances few hundred meters away from the spacecraft are conceivable. For instance, two sets of this AI pairs at different distances d and d' (Figure 15) outsize the gray region can distinguish the acceleration due to the offset $\gamma\ \delta d$ and due to non-gravitational forces δa acting on the retroreflection mirror. Following the argument in the previous paragraph, the mean accelerations for AI pairs at two locations are $a_m(d, d') = -\delta a + (\gamma(d, d') + \gamma_G)\delta$, respectively. Note that δd and δa are identical to all AIs, since all of them are driven from the same laser pulses and preferably from the same cloud. Due to the difference of $\gamma(d)$ and $\gamma(d')$, the difference $a_m(d) - a_m(d') = \big(\gamma(d) - \gamma(d')\big)\delta d$ vanishes only if $\delta d = 0$. Thus, δd can be controlled slowly and actively to meet the demanded acceleration resolution, without operating AIs in regions of small γ. It should be pointed out that, while additional AI measurements add some complexity to the operation, the all atom clouds can be from the same source and their AI operations use the same set of the lasers. It does not therefore add much more complexity in the hardware implementation.

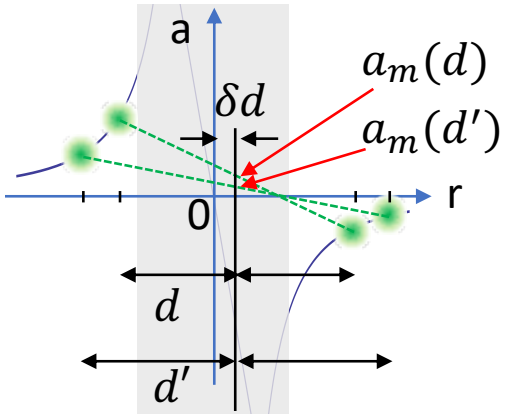

Figure 15. Depiction of self-gravity gradient suppression with four AIs (green balls). Deviation δd of the mean position of the AIs from the CM (r=0) will lead to $a_m(d) \neq a_m(d')$. Minimizing $a_m(d) - a_m(d')$ actively will reduce the self gravity gradient error below the required accuracy.

4.3 Laser ranging interferometry

LRI uses a stable laser as a ruler for precise distance measurements between spacecraft. The concept has been developed and matured in the GRACE Follow-On (GRACE-FO) mission launched in 2018, and to be implemented in the planned LISA mission. Current technology capability of LRI can be summarized in the mission requirements: The LRI requirement for GRACE-FO is 80 nm$/\sqrt{\text{Hz}}$ above 10 mHz with a 2×10^5 m baseline and that for LISA is ~12 pm$/\sqrt{\text{Hz}}$ above 1 mHz with a 2.5×10^9 m arm length [35].

The baseline L of the tetrahedral formation, though pending on trade-off studies between systematic and sensitivity, will most likely be on the order of 10^6 m (compared to the LISA laser arm length of 1x10^9 m). The gradient sensitivity target of 10^{-24} /s^2 manifests as differential acceleration of $10^{-24} \times L$ m/s^2. Note that GODDESS mission requires the stability of the acceleration measurement over the mission life span of 3 years, and thus the optical frequency long-term stability is also critical. Taking L=10^6 m as an example, the acceleration resolution is 10^{-18} m/s^2, which is ~1 μm after 3 years. Thus, the laser frequency needs to have fractional

stability of 10^{-12} over 3 years. The lasers in GRACE-FO and LISA are referenced to ultra-stable cavities meeting the corresponding mission requirements for the measurement time of 1,000 s or less, thus the long-term stability (below mHz in the Fourier frequency domain) is not required and not maintained. For the year-long time scale, frequency stabilities are maintained with atomic frequency references by locking the laser frequency to an appropriate atomic transition. In the field of optical frequency standard, accuracy of $1\text{x}10^{-17}$ or lower are being pushed. Thus, the required stability floor of $1\text{x}10^{-12}$ is achievable without much difficulty.

Pointing is less a concern in terms of systematics, since the relative angles are calculated from the arm lengths. Acquiring and maintaining lock of LRI between spacecraft is not more challenging than LISA simply due to shorter arm lengths in the measurement concept. With the success of GRACE-FO and LISA mission on the way, the relevant technologies needed for the GODDESS mission have no foreseen impossible technical obstacles.

5. Other possible science measurements and significance

The GODDESS mission concept design is focused on the direct detection of dark energy field. Since the detection of the Vainshtein field force formulated is in a form of the test of the inverse square law, it will be interesting to compare it to the other existing ISL tests. The inverse square law has been tested in wide length scale ranges, and is typically parametrized in Yukawa parameters, α and λ. The Yukawa potential, $V(r) = -GM/r\left(1 + \alpha e^{-\frac{r}{\lambda}}\right)$, modifies the gravitational potential by an additional exponentially decaying term. Thus, the Laplacian (that is, the trace of the force field tensor) of Yukawa potential does not vanish. From the galileon measurement sensitivities discussed in the mission concept, GODDESS can place similar constraints on the Yukawa potential parameters. Figure 16 shows the parameter regions that have been excluded by the existing laboratory experiments and solar observations so far [39]. The blue region indicates the parameters for Yukawa Laplacian ≥ 10^{-24} /s^2 at 1 AU. Thus, the proposed mission (blue region) will improve the ISL by at least an order of magnitude for distances larger than 0.1 AU. It is important to point out, however, and to the best of our knowledge, that there has been no established constraint on Vainshtein model from solar observations. While such constraints are possible, it requires some careful analysis and cannot be simply inferred from the ISL tests.

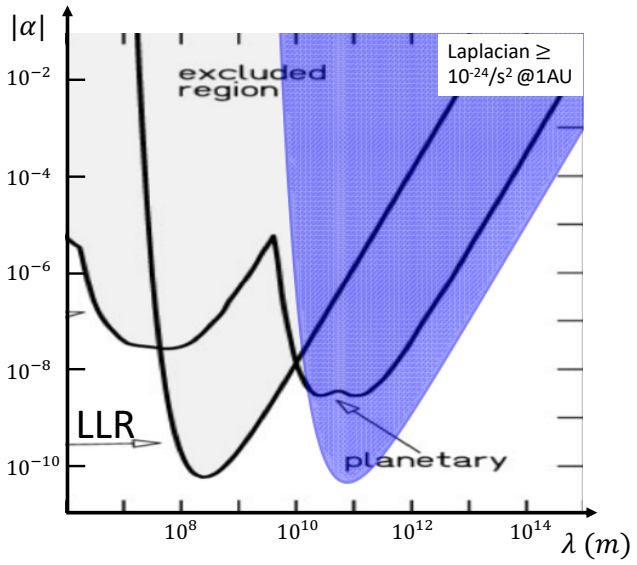

Figure 16. Exclusion plot of Yukawa parameters. LLR: lunar laser ranging. Colored region is parameters for Yukawa Laplacian greater than the galileon Laplacian.

The measurement experiment data set from the arms of the tetrahedron formation, although designed to measure the solar galileon, is rich for other astrophysical and fundamental physics

studies. For instance, the cosmological constant $\Lambda \simeq 10^{-52}$ /m^2, though currently not a preferred explanation of the accelerated expansion of the universe, has a weak-field-limit potential $\phi_\Lambda = -\Lambda c^2 r^2/6$ on the local scale and a non-vanishing Laplacian $c^2\Lambda \sim 10^{-35}$ /s^2, independent of the distance R to the Sun [40]. The Laplacian is currently constrained to $<10^{-24}$ /s^2 based on bounds of Λ placed by observation of planetary orbits. Since the Laplacian of galileon decreases as $\sim R^{-3/2}$ while the Laplacian of ϕ_Λ is constant across the solar system, the dependence of tracelessness to R will eventually distinguish between the two theories even in the case where the Laplacian of galileon theories or alike is similar to $\nabla^2\phi_\Lambda$. Extending to more general terms, every dark energy theory is fundamentally a modified gravity model that violates the ISL and predicts a non-vanishing trace of the gradient tensor. The tracelessness test is thus *a universal model independent probe scheme* to all dark energy and modified gravity theories.

Furthermore, the tracelessness of gravitational gradient tensor holds in regions of no mass density. Dark matter, on the other hand, would contribute an average background density $\rho_m \sim 10^{-21}$ kg/m^3 and $\nabla^2\phi_G = 4\pi G\rho_m \sim 10^{-31}$ /s^2 [41] [42]. The experiment data from all cross link differential measurements can be potentially used to analyze and detect (or constrain) dark matter, perhaps in the forms of time/space dependent clumps or waves or some background density in the solar system.

Last but not the least, the satellite formation shown in Figure 7 is obviously sensitive to gravitational waves. Indeed, every three of the four spacecraft forms a LISA-like triangular constellation, which uses laser ranging between inertial references, and thus are sensitive to gravitational waves. With four triangles facing different directions, the tetrahedral formation measures not only gravitational waves, but also their propagation directions, stochastic gravitational waves, and provide redundancy in gravitational wave data. Interestingly, the optimal baseline lengths for the galileon fields are likely shorter than the LISA intended baseline length. In the case, the galileon detector would be a very sensitive mid-band gravitational wave detector, covering the spectrum gap between LIGO and LISA where the astrophysical science is believed to be rich and abundant [24] [36].

6. Summary

In this NIAC study, we showed at the concept level that it is scientifically and technically feasible to detect the galileon signals of the dark energy field directly in a solar system mission. Such a mission would not only shine light on the nature of dark energy, but also provide invaluable data for testing any gravity field theory in general beyond the Newtonian gravity, hunting for ultra-light fields of dark matter, as well as gravitational wave detections in the mid band frequency spectrum.

It is clear that realizing the mission concept is very technically challenging. Indeed, it is a mission with the technical sophistication and complexity beyond LISA in laser ranging, drag-free control and spacecraft formation flight. Suppressing the gravity effects by 10 orders of magnitude is at the heart of the challenge for the direct dark energy detection. With the proposed detection strategy of measuring the trace of the field force gradient tensor, the gravity effects can be completely eliminated in principle, and the focus can be on controlling and reducing systematic errors in the measurements. We also showed that the measurement sensitivity could be further improved by reducing high-order systematics from the gravity effects with correction coefficient

measurements. On the other hand, systematics from the measurement instrument itself must be significantly better controlled and actually much smaller than those demonstrated on the ground thanks to the more benign space microgravity environment far away from the Earth and much of the common mode rejection schemes used.

It is important to point out that the mission architecture design itself plays a significantly role in reducing measurement systematics. For example, one of the main difficulties in the trace measurement scheme is the fact that the dark energy signal is at DC to the first order, the test of a non-zero trace. Any measurement at DC is prone to errors due to biases and drifts. If one can modulate the dark energy signal, the detection would be at a higher frequency to remove potential biased and drifts. This can be done through a better understanding of the spatial variations of the dark energy signal in the solar system and design of the mission measurement orbits accordingly.

Because of the potential significant impact to the mission concept, we have jump-started an effort of dark energy field simulation to gain the understanding and knowledge of the field affected by the solar massive bodies. Due to the highly nonlinear equation of state of galileon fields, numerical simulations tend to be unstable or contain artifacts. Galileon signals have been estimated based on the analytical solution of a spherical body, and the measurement strategy has been staying away from planets such that the galileon is dominated by the Sun. However, there may exist regions of signal enhancement in 2-body or 3-body settings, and signal modulations may come naturally as suggested in the concept description section. A reliable three-dimensional numerical simulation package for arbitrary mass distribution will help better define mission concept, mission requirements, and estimate science return.

In this study, we have identified key technologies that enable the concept of direct detection of the galileon dark energy in the solar system. The key enabler is the atomic test masses that can be operated in free space vacuum away from the spacecraft. Atomic test masses, operated in the form of atomic interferometers, provide the necessary measurement stabilities required for such a measurement endeavor. Most of the required atom interferometer operation schemes, including atom transport, large-momentum transfer atom optics, and differential measurements have been demonstrated in the research labs, with the exception of the high-flux high-speed BEC production. The required flux of the ultra-cold atoms from an BEC source is about 2 orders of magnitude higher than what has been shown in laboratories. There are paths to achieve it but it remains to be demonstrated. Operation of atom interferometers in free space vacuum will need to be demonstrated, and requires perhaps a technology demonstration mission in space for the proof of concept and maturation. A cislunar gateway would be a suitable platform for such demonstration.

Use of the laser ranging interferometer for the gravity differential measurements is akin to that in LISA. The basic laser interferometer ranging is already being demonstrated in the NASA GRACE-FO mission. The laser ranging required for the dark energy measurement is more stringent than that of GRACE-FO and even that of LISA. Moreover, the high precision gradiometer measurement required the high precision of the absolute ranging measurement at micro meter level which is being routinely done in laboratory scale. One does not expect any unsurmountable challenge in meeting such a requirement but needs demonstrated and validated over the long distance for absolute ranging measurements.

In summary, we have developed a measurement scheme and the GODDESS mission concept capable of direct detection of dark energy, particularly for the cubic galileon of the Sun. Based on the first order estimates of the signal size, instrument performance, we showed that the mission

concept is sound and measurement techniques are feasible. We identified certain areas of technology that need to be advanced or demonstrated for a mission realization. With continued development and refinement of the mission concept, and proper technology maturation development supports, it is conceivable to realize such a mission in the next 15 to 20 years. GODDESS will decisively validate or disprove cubic galileon theory in 3 years, and at the same time, contribute to constrain cosmological constant, detect dark matter ultra-light field, and detect gravitational waves. The mission will be able to help answer the most fundamental and mysterious question about fundamental physics, astrophysics and cosmology.

7. Acknowledgement

This work was performed at the Jet Propulsion Laboratory, California Institute of Technology, under a contract with the National Aeronautics and Space Administration.

Government sponsorship acknowledged.

8. Institution Required Disclaimer

This report contains Pre-Decisional Information -- For Planning and Discussion Purposes Only

9. References

[1] E. J. Copeland, M. Sami and S. Tsujikawa, "DYNAMICS OF DARK ENERGY," *International Journal of Modern Physics D,* vol. 15, pp. 1753-1935, 2006.

[2] A. Joyce, B. Jain, J. Khoury and M. Trodden, "Beyond the cosmological standard model," *Physics Reports,* vol. 568, pp. 1-98, 2015.

[3] S.-w. Chiow and N. Yu, "Multiloop atom interferometer measurements of chameleon dark energy in microgravity," *Physical Review D,* vol. 97, p. 044043, 2018.

[4] M. Jaffe, P. Haslinger, V. Xu, P. Hamilton, A. Upadhye, B. Elder, J. Khoury and H. Müller, "Testing sub-gravitational forces on atoms from a miniature in-vacuum source mass," *Nature Physics,* vol. 13, pp. 938-942, 2017.

[5] B. Elder, J. Khoury, P. Haslinger, M. Jaffe, H. Müller and P. Hamilton, "Chameleon dark energy and atom interferometry," *Phys. Rev. D,* vol. 94, no. 4, p. 044051, 8 2016.

[6] P. Hamilton, M. Jaffe, P. Haslinger, Q. Simmons, H. Müller and J. Khoury, "Atom-interferometry constraints on dark energy," *Science,* vol. 349, pp. 849-851, 2015.

[7] P. Haslinger, M. Jaffe, V. Xu, O. Schwartz, M. Sonnleitner, M. Ritsch-Marte, H. Ritsch and H. Müller, "Attractive force on atoms due to blackbody radiation," *arXiv preprint arXiv:1704.03577,* 2017.

[8] J. Sakstein, "Tests of Gravity with Future Space-Based Experiments," *arXiv preprint arXiv:1710.03156,* 2017.

[9] P. Creminelli and F. Vernizzi, "Dark Energy after GW170817 and GRB170817A," *Physical Review Letters,* vol. 119, 12 2017.

[10] M. Crisostomi and K. Koyama, "Vainshtein mechanism after GW170817," *Physical Review D,* vol. 97, 1 2018.

[11] P. R. Berman and V. Kharchenko, *Atom interferometry,* AIP, 1997.

[12] M. Kasevich and S. Chu, "Atomic interferometry using stimulated Raman transitions," *Physical review letters,* vol. 67, p. 181, 1991.

[13] H. Müller, S.-w. Chiow and S. Chu, "Atom-wave diffraction between the Raman-Nath and the Bragg regime: Effective Rabi frequency, losses, and phase shifts," *Physical review A,* vol. 77, p. 023609, 2008.

[14] *http://www.nobelprize.org/nobel_prizes/physics/laureates/2001/.*

[15] W. Ketterle, D. S. Durfee and D. M. Stamper-Kurn, "Making, probing and understanding Bose-Einstein condensates," 2 4 1999.

[16] A. Peters, K. Y. Chung and S. Chu, "High-precision gravity measurements using atom interferometry," *Metrologia,* vol. 38, p. 25, 2001.

[17] S.-w. Chiow, J. Williams and N. Yu, "Laser-ranging long-baseline differential atom interferometers for space," *Physical Review A,* vol. 92, 12 2015.

[18] S.-w. Chiow, T. Kovachy, H.-C. Chien and M. A. Kasevich, "102ℏkLarge Area Atom Interferometers," *Physical Review Letters,* vol. 107, 9 2011.

[19] T. Kovachy, P. Asenbaum, C. Overstreet, C. A. Donnelly, S. M. Dickerson, A. Sugarbaker, J. M. Hogan and M. A. Kasevich, "Quantum superposition at the half-metre scale," *Nature,* vol. 528, pp. 530-533, 12 2015.

[20] T. Kovachy, J. M. Hogan, A. Sugarbaker, S. M. Dickerson, C. A. Donnelly, C. Overstreet and M. A. Kasevich, "Matter Wave Lensing to Picokelvin Temperatures," *Physical Review Letters,* vol. 114, 4 2015.

[21] J. Rudolph, W. Herr, C. Grzeschik, T. Sternke, A. Grote, M. Popp, D. Becker, H. Müntinga, H. Ahlers, A. Peters, C. Lämmerzahl, K. Sengstock, N. Gaaloul, W. Ertmer and E. M. Rasel, "A high-flux BEC source for mobile atom interferometers," *New Journal of Physics,* vol. 17, p. 065001, 6 2015.

[22] D. Becker, M. D. Lachmann, S. T. Seidel, H. Ahlers, A. N. Dinkelaker, J. Grosse, O. Hellmig, H. Müntinga, V. Schkolnik, T. Wendrich, A. Wenzlawski, B. Weps, R. Corgier, T. Franz, N. Gaaloul, W. Herr, D. Lüdtke, M. Popp, S. Amri, H. Duncker, M. Erbe, A. Kohfeldt, A. Kubelka-Lange, C. Braxmaier, E. Charron, W. Ertmer, M. Krutzik, C. Lämmerzahl, A. Peters, W. P. Schleich, K. Sengstock, R. Walser, A. Wicht, P. Windpassinger and E. M. Rasel, "Space-borne Bose–Einstein condensation for precision interferometry," *Nature,* vol. 562, pp. 391-395, 10 2018.

[23] B. Barrett, L. Antoni-Micollier, L. Chichet, B. Battelier, T. Lévèque, A. Landragin and P. Bouyer, "Dual matter-wave inertial sensors in weightlessness," *Nature Communications,* vol. 7, 12 2016.

[24] J. M. Hogan, D. M. S. Johnson, S. Dickerson, T. Kovachy, A. Sugarbaker, S.-w. Chiow, P. W. Graham, M. A. Kasevich, B. Saif, S. Rajendran and others, "An atomic gravitational

wave interferometric sensor in low earth orbit (AGIS-LEO)," *General Relativity and Gravitation,* vol. 43, pp. 1953-2009, 2011.

[25] D.-F. Gao, J. Wang and M.-S. Zhan, "Atomic Interferometric Gravitational-Wave Space Observatory (AIGSO)," *Communications in Theoretical Physics,* vol. 69, p. 37, 1 2018.

[26] *http://sci.esa.int/ste-quest/.*

[27] S.-w. Chiow, J. Williams and N. Yu, "Noise reduction in differential phase extraction of dual atom interferometers using an active servo loop," *Physical Review A,* vol. 93, p. 013602, 2016.

[28] *https://catalog.data.gov/dataset/cold-atom-gravity-gradiometer-for-geodesy.*

[29] S.-w. Chiow and N. Yu, "Compact atom interferometer using single laser," *Applied Physics B,* vol. 124, 5 2018.

[30] *https://www.nasa.gov/spacetech/niac/2013phaseII_saif.html.*

[31] *http://coldatomlab.jpl.nasa.gov.*

[32] T. Hiramatsu, W. Hu, K. Koyama and F. Schmidt, "Equivalence principle violation in Vainshtein screened two-body systems," *Physical Review D,* vol. 87, 3 2013.

[33] E. V. Pitjeva, "Determination of the Value of the Heliocentric Gravitational Constant (GM⊙) from Modern Observations of Planets and Spacecraft," *Journal of Physical and Chemical Reference Data,* vol. 44, p. 031210, 9 2015.

[34] J. M. Hogan and M. A. Kasevich, "Atom-interferometric gravitational-wave detection using heterodyne laser links," *Physical Review A,* vol. 94, 9 2016.

[35] M. Armano, H. Audley, J. Baird, P. Binetruy, M. Born, D. Bortoluzzi, E. Castelli, A. Cavalleri, A. Cesarini, A. Cruise, K. Danzmann, M. Deus Silva, I. Diepholz, G. Dixon, R. Dolesi, L. Ferraioli, V. Ferroni, E. Fitzsimons, M. Freschi, L. Gesa, F. Gibert, D. Giardini, R. Giusteri, C. Grimani, J. Grzymisch, I. Harrison, G. Heinzel, M. Hewitson, D. Hollington, D. Hoyland, M. Hueller, H. Inchauspé, O. Jennrich, P. Jetzer, N. Karnesis, B. Kaune, N. Korsakova, C. Killow, J. Lobo, I. Lloro, L. Liu, J. López-Zaragoza, R. Maarschalkerweerd, D. Mance, N. Meshksar, V. Martín, L. Martin-Polo, J. Martino, F. Martin-Porqueras, I. Mateos, P. McNamara, J. Mendes, L. Mendes, M. Nofrarias, S. Paczkowski, M. Perreur-Lloyd, A. Petiteau, P. Pivato, E. Plagnol, J. Ramos-Castro, J. Reiche, D. Robertson, F. Rivas, G. Russano, J. Slutsky, C. Sopuerta, T. Sumner, D. Texier, J. Thorpe, D. Vetrugno, S. Vitale, G. Wanner, H. Ward, P. Wass, W. Weber, L. Wissel, A. Wittchen and P. Zweifel, "Beyond the Required LISA Free-Fall Performance: New LISA Pathfinder Results down to 200.167em0.167emHz," *Physical Review Letters,* vol. 120, 2 2018.

[36] P. W. Graham, J. M. Hogan, M. A. Kasevich, S. Rajendran and R. W. Romani, "Mid-band gravitational wave detection with precision atomic sensors," 6 11 2017.

[37] J. Hu, A. Urvoy, Z. Vendeiro, V. Crépel, W. Chen and V. Vuletić, "Creation of a Bose-condensed gas of87Rb by laser cooling," *Science,* vol. 358, pp. 1078-1080, 11 2017.

[38] B. Estey, C. Yu, H. Müller, P.-C. Kuan and S.-Y. Lan, "High-Resolution Atom Interferometers with Suppressed Diffraction Phases," *Physical Review Letters,* vol. 115, 8 2015.

[39] E. G. Adelberger, B. R. Heckel and A. E. Nelson, "TESTS OF THEGRAVITATIONALINVERSE-SQUARELAW," *Annual Review of Nuclear and Particle Science,* vol. 53, pp. 77-121, 12 2003.

[40] M. Sereno and P. Jetzer, "Solar and stellar system tests of the cosmological constant," *Physical Review D,* vol. 73, 3 2006.

[41] T. Kalaydzhyan and N. Yu, "Extracting dark matter signatures from atomic clock stability measurements," *Physical Review D,* vol. 96, 10 2017.

[42] T. Kalaydzhyan and N. Yu, "Searching for Stochastic Background of Ultra-Light Fields with Atomic Sensors," *Universe,* vol. 4, p. 99, 9 2018.